Control of wave energy devices


Taylor & Francis
Taylor & Francis Group
http://taylorandfrancis.com

Developments in Renewable Energies Offshore – Guedes Soares (Ed.)

Black-box modelling of a three-body hinge-barge wave energy device via forces responses

F. Jaramillo-Lopez & J. Ringwood*
Centre for Ocean Energy Research (COER), Maynooth University, Co. Kildare, Ireland

B. Flannery & J. Murphy
Department of Civil and Environmental Engineering, University College Cork, Co. Cork, Ireland

ABSTRACT: Effective modelling of Wave Energy Converters (WEC) is fundamental in the design and implementation of power-maximizing controllers. It is possible to get accurate dynamic models with system identification techniques based on experimental input-output data. However, even though these techniques are well developed in other application areas they are seldom used in the context of WECs. This work describes the methodology used to model a three-body hinge-barge wave energy device using experimental data. Some identification strategies are discussed to get a linear time-invariant dynamic model. The obtained model is validated against a data set separate from that used for identification, to ensure the generalisation capabilities of the model.

1 INTRODUCTION

Global concerns over climate change has resulted in new policies and regulations that have stimulated the interest in alternative energy sources. A wave energy converter is a system that captures energy from ocean waves. In order to compete with other energy systems, WEC systems have to overcome many challenges. One of these challenges is to absorb the maximum time average power from the ocean, which can be greatly assisted by constructing effective dynamic models and designing power-maximizing controllers. In (Ringwood et al. 2014) and (Ringwood 2020), an overview is given about the state of technology development for WEC models and control systems.

The efficacy of power-maximizing controllers is closely related to the WEC dynamical models that they use. WEC models can be classified mainly into three categories, depending on which techniques are used to get the model (other generalized classifications can be found in (Ljung 2010)):

- White-box models. Based only on physical considerations, i.e., hydrodynamic modelling.
- Black-box models. Based only on system identification (SI) techniques.
- Grey-box models. Combination of hydrodynamic modelling and SI techniques.

Hydrodynamic models, in the wave energy field, are generally based in linear potential theory (LPT), which assumes inviscid fluid, irrotational flow, small waves and small body motion. These models use Cummin's equation (Cummins 1962), which is derived using LPT and Newton's second law:

$$(m + m_\infty)\ddot{x}(t) + \int_0^t K_r(t-\tau)\dot{x}(\tau)d\tau + S_h x(t) = f_I \tag{1}$$

where m and m_∞ are the mass and the infinite frequency added mass of the system, respectively, K_r is the radiation impedance impulse response, S_h is the hydrostatic stiffness and $f_I = f_m + f_e + f_{PTO}$, with $\mathrm{f_m}$ the mooring forces, f_e the excitation force from the fluid and f_{PTO} (also denoted as f_u) the control force applied by a power take off (PTO) system. $x(t)$, $\dot{x}(t)$ and $\ddot{x}(t)$ denote the body displacement, velocity, and acceleration, respectively.

In (O'Cathain et al. 2007), an analytical approach for modelling multibody wave energy devices is presented. The Newton-Euler equations with eliminated constraints are utilized to capture the rigid body dynamics of the constrained multibody system. In a recent study, Paparella et al. (2016) presents two different analytical formulations to describe the dynamics of multibody systems. The results are validated with experimental tests using a three-body hinge-barge device as a case study. The same WEC is analyzed in

* This paper is based upon work supported by Science Foundation Ireland under Grant no. 13/IA/1886

(Paparella and Ringwood 2017), but this time, the authors focus on the optimal control problem, which takes into account physical constraints.

Several works have been reported to increase the accuracy of linear hydrodynamic models by identifying some of their terms, or by adding nonlinear terms (see Giorgi et al. 2019 and references therein). They apply SI techniques to get the terms and obtain so-called grey-models. In addition, there are reported works that have extended the use of SI techniques from the identification of specific hydrodynamic terms to the complete dynamic model (black-box models), see also (Giorgi et al. 2019) for a detailed review of related works.

In this work, a complete (black-box) dynamic model for a three-body hinge-barge wave energy device is derived using SI techniques. Several strategies are presented to get an accurate linear model. The derived model is tested on unseen data, i.e., on a validation data set separate from that used for SI.

The remainder of the paper is organized as follows. Section 2 presents the fundamentals of system identification applied to wave energy devices. A detailed description of the case study of this work is presented in Section 3. Section 4 introduces the main results of this paper. It details the strategies developed to get the estimated linear model, while model validation is also discussed in this Section. Finally, Section 5 is devoted to conclusions.

2 SYSTEM IDENTIFICATION

The system identification methodology consists of the following steps (Davidson et al. 2016):

- a parametric structure is chosen for the model,
- a suitable input signal, $u(t)$ is synthesized and input to the experimental system,
- the input signal, $u(t)$ and resulting output signal, $y(t)$ are recorded,
- an identification algorithm is used to determine the optimal parameter vector, which minimizes some error metric between the actual measured output $y(t)$ and that produced by the identified parametric model $\hat{y}(t|\theta)$.

The most usual way to identify models is by using input and output time signals (time-domain data): $Z^N = \{u(1), y(1), \ldots, u(N), y(N)\}$. A continuous-time linear time-invariant model can be written as

$$G(s,\theta) = \frac{b_0 s^m + b_1 s^{m-1} + \cdots + b_m}{s^n + a_1 s^{n-1} + \cdots + a_n} \tag{2}$$

where s is the Laplace variable, and θ are the model parameters: $b_0 \ldots b_m$ and $a_1 \ldots a_n$. The simulated output for a particular set of parameters can be defined as follows:

$$\hat{y}(t|\theta) = G(p,\theta)u(t) \tag{3}$$

where p denotes the differentiation operator. The parameters are then estimated by minimizing the loss function $J(\theta)$ (also denoted as the error metric) (Giorgi et al. 2019, Ljung 2002, Ljung 2009, Ljung 1999, Ljung 2019):

$$\hat{\theta}_N = \arg\min_{\theta} J(\theta). \tag{4}$$

The error metric used in this work is the Normalized Root Mean Squared Error (NRMSE) (Ljung 2019):

$$J(\theta) = NRMSE = \frac{\sum_{t=1}^{N} \| y(t_k) - \hat{y}(t_k|\theta) \|}{\sum_{t=1}^{N} \| y(t_k) - \bar{y}(t_k) \|} \tag{5}$$

where $y(t_k)$ is the discrete time measured output data, $\bar{y}(t_k)$ is its mean, and $\hat{y}(t_k|\theta)$ is the discrete time predicted response of the model.

It is also possible to identify continuous-time transfer function models from frequency domain data when the input-output data are given in the frequency domain as Fourier transforms (see (see Ljung 1999, Section. 7.7 and Ljung 2002, Ozdemir and Gumussoy 2017). In (Ozdemir and Gumussoy 2017), In (Ozdemir and Gumussoy 2017), the authors describe the methodology to follow in such a case. In this last work, we can note that the identification procedure not only is quite different from the time-domain case, but also diverse issues may be found in this methodology, such as numerical issues or lack of convergence to a local minimum.

Some works have been proposed that use the frequency domain estimation methodology to identify discrete-time transfer function models, such as the work presented in (Garcia-Violini et al. 2020). In that work, the authors estimate the transfer function for a single-body WaveStar wave energy converter with a single operational degree of freedom in pitch. Then, using the identified model, an LTI energy maximising controller is developed. A set of observed data from a numerical WEC-Sim model: $W^n = \{u(1), y(1), \ldots, u(n), y(n)\}$ where each element corresponds to an experiment with an input signal with same shape but different amplitude was utilized to compute their Fourier transforms and then estimate a set of empirical transfer functions - one estimate for each experiment; i.e.,

$$\hat{H}_n(j\omega) = \frac{Y_n(j\omega)}{U_n(j\omega)} \tag{6}$$

where $\hat{H}_n$ is the nth empirical transfer function estimate (ETFE), Y_n and U_n are the frequency responses

of the nth output and input signals, respectively. Then, the averaged frequency response (AFR) $\bar{H}(j\omega)$ is calculated by averaging the frequency response of all of the ETFEs. This is done to build a low-variance data set. After that, the methodology described in (Ljung 1999, Section. 7.7) and (Ozdemir and Gumussoy 2017) is used to obtain the discrete-time transfer function estimate $\hat{G}_0(j\omega)$ using the AFR $H(j\omega)$ as primary data.

In the context of wave energy, the recorded data for system identification can be originated from two sources: real tank (RT) tests and numerical wave tank (NWT) simulations. NWT can be implemented using boundary-element methods or computational fluid dynamics (CFD). CFD-based NWTs offer fully nonlinear hydrodynamic calculations by solving the Navier-Stokes equations. In (Davidson et al. 2016) and (Giorgi et al. 2016) the authors describe advantages and disadvantages of RT and NWT. In this work, we use RT tests to gather the data for the identification process. In Section 3, a detailed description of the data logging setup is given.

Depending on the forces applied to excite the system (see Figure 1), it is possible to obtain two different WEC models (Davidson et al. 2016): free surface elevation (FSE) to body motion, and input force to body motion. In the former case, wave excitation experiments — which produce the fluid excitation forces f_e — are used to provide two time series vectors, one containing the FSE (the input) and the other the body displacement (the output). In the latter case, input force experiments (f_u) are used to identify the model. Two time series vectors are produced by these experiments: one containing the input force (the input) and the other the body displacement (the output). In the present work, we use the input force to body motion approach, where the input force is given by the PTO system f_u, while the excitation and the mooring forces are zero, i.e., $f_e = 0$ and $f_m = 0$, respectively. The main advantage of using this forced (PTO) response approach is that it allows total freedom over the choice of input signal to be applied to the system and can elicit responses and fluid structure interactions beyond those achievable with wave excitation alone. In this regard, it is important to ensure that the input signal covers the frequency range of interest and that input power is applied to the parts of the spectrum where the identified model is required to perform well (Davidson et al. 2016).

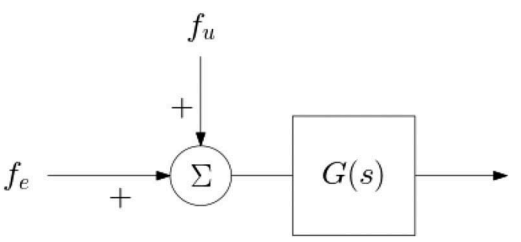

Figure 1. Forces applied to wave energy converters.

This work, where SI techniques are used to get a representative linear model, follows the notions presented in (Davidson et al. 2015).

3 CASE STUDY

The system under study in this work is a three-body hinge-barge wave energy converter. Figure 2 shows the hinge-barge (HB) device which consists of the fore, central and aft bodies, two linear motors with 250 N max. force capacity manufactured by LinMot, two load cells connected to the motors to measure the applied forces, and two rotary encoder sensors to measure the relative angles between the fore and central, and between the aft and central bodies. The experiments were conducted in this device by applying a set of excitation signals to each motor, separately, and recording the angles of both encoders. The data logging setup is shown in Figure 3. It consist of rotary encoder and load cell sensors, a data acquisition system (DAS), a main computer to control the DAS, another computer to control the originated waves and the wave tank itself, which dimensions are 25 m x 15 m x 1 m deep. The main computer uses dSpace to compile the models and to control the DAS.

The HB device belongs to the attenuator class of devices. Other hinge barge devices include the M-Ocean (Mocean Energy 2020), M4 device (Stansby et al. 2015) as well as other devices which achieved some degree of deployment such as Seapower (Seapower 2020) deployed in Galway bay 2016, the McCabe Wave Pump (deployed in the Shannon estuary in 1996) and perhaps, most famously, the Pelamis device (Yemm et al. 2012).

Indeed, the three-bodied device in this study is the direct descendant of the original McCabe Wave Pump. The original McCabe wave pump consisted of three rectangular steel pontoons, which are hinged together across their beam. The pontoons move relative to each other with the waves. A damper plate is attached to the central pontoon, which ensures that it stays still as the fore and aft pontoons move relative

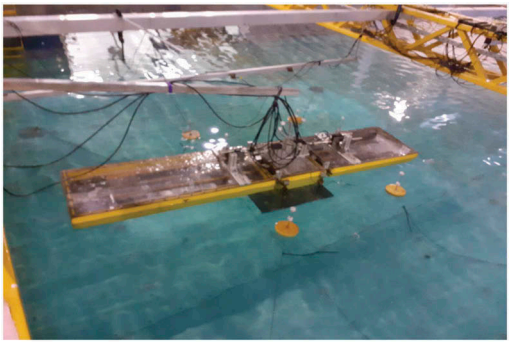

Figure 2. Three-body hinge-barge wave energy converter.

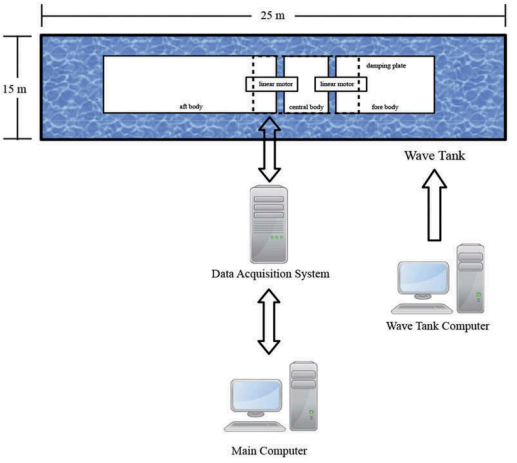

Figure 3. Wave tank and data logging setup.

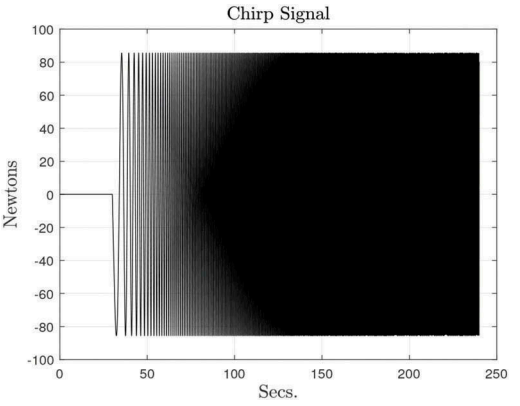

Figure 4. Chirp signal with frequency swept from 0.5 to 8 rad/s and 85 N amplitude.

to the central pontoon by pitching about the hinges. Energy is extracted from the rotation about the hinge points by linear hydraulic pumps mounted between the central and two outer pontoons near the hinges (de Almeida and Moura 2007).

The current 1:20 scale device was built by the Wave Energy Conversion Corporation of America (WECCA) (who also submitted a 1:50 scale model for the wave energy prize (Offshore Energy 2016). The device was significantly modified as part of the current BenchWEC project with the addition of two PS01-37x120F-HP-C LinMot motors so that advanced modelling and control techniques could be investigated.

4 RESULTS

The model structure chosen for the identification process is a continuous-time linear time invariant structure. This is the most simple model structure; nevertheless, it has significant precedent due to the number of linear controllers for WECs available in the literature. As stated in Section 2, the input excitation signal should cover the whole range of frequencies and amplitudes of the normal system operation in order to get a model with ability to be consistent on new experiments. In this regard, wave excitation tests were conducted to get the natural resonance frequency of the HB device, and this information was used to establish the operational range of frequencies of the device. A set of chirp signals was used for input excitation, with a linear frequency sweep from 0.5 to 8 rad/s, and five different amplitudes: $IES = \{37, 53, 85, 102, 134\}$ N. Figure 4 shows a chirp signal with an 85 N amplitude.

4.1 *Data preprocessing*

Experimental data may have flaws of several types due to many reasons such as uncalibrated sensors (offsets), leading and/or trailing null information (for synchronization purposes), different sample periods between inputs and outputs, non-constant sample period in the same input and/or output set, and missing information (due to other demanding tasks in the operating system); thus, it is necessary to do some data preprocessing to alleviate these problems to the greatest extent possible. Figure 5 shows some of the problems found in the recorded data for the HB WEC.

Graph a) in Figure 5 shows the angle measurements in the aft barge sensor with a chirp input signal of 85 N amplitude applied to the aft linear motor. Notice the offset of this signal (around -8º), and the leading and trailing null information. In graph b) of the same figure, there are two segments of missing information in the force measurements of the fore body. The input excitation is a chirp signal with an amplitude of 53 N applied to the fore linear motor. Each segment has missing information of around one second duration; with a 1/1000 sample period, about 1000 samples are lost in each segment.

4.2 *Linear model estimation*

The first step in the model identification process was to establish if the system can be approximated with a linear model as opposite to a nonlinear model. In this respect, the ETFE of each experiment data set was calculated as shown in (6). Figure 6 shows the frequency response for each ETFE. It can be noticed that the models have a similar frequency response, except for some of the smaller input signal amplitudes, i.e., 37 and 53 N. This is due to the lower signal-to-noise ratios for these signals.

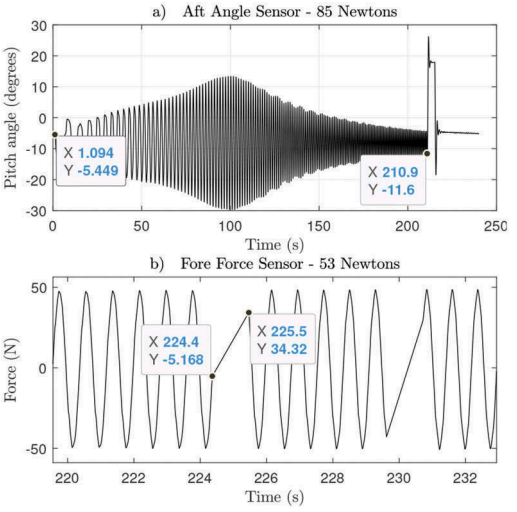

Figure 5. Problems found in the experimental data.

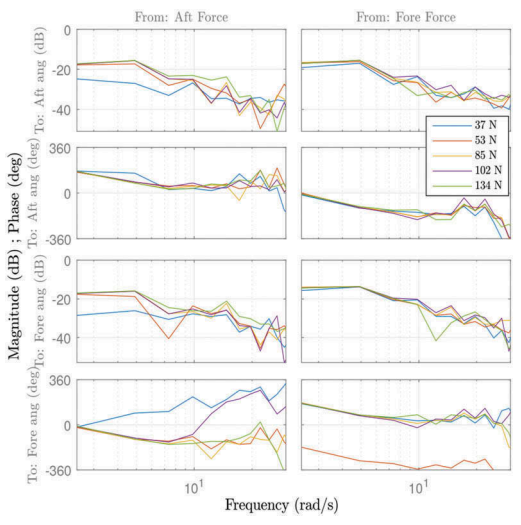

Figure 6. Empirical transfer function estimates.

In order to get an accurate linear model, several identification strategies were used. They are described as follows.

1. Calculate the ETFE for each input excitation signal in the set IES, and then calculate the averaged frequency response of all of the ETFEs. The identified model is calculated by using frequency domain SI techniques that employ the averaged frequency response as primary data. Note that this is the same methodology employed in (Garcia-Violini et al. 2020) and it is fully described in Section 2.
2. Estimate the continuous transfer function for each input excitation signal in the set IES using time-domain SI techniques and then calculate a global estimate using a weighting sum of each estimated transfer function.
3. Merge the data for all the recorded input and output signals and then estimate the continuous transfer function with these merged data, using time-domain SI techniques. When estimating the transfer function in this way, the prediction error vector is formed over the entire collection of experiments, assigning equal weight to observations in each experiment, i.e., the identification is done using all the input and output signals of the five experiments at the same time.

Each identification strategy produced a transfer function matrix (TFM) $\hat{H}_i(s)$, which consists of 2x2 elements, where each element in the matrix corresponds to a transfer function between each input signal (aft and fore forces) and each output signal (aft and fore angles):

$$\hat{H}_i(s) = \begin{bmatrix} \frac{\hat{Y}_1(s)}{\hat{U}_1(s)} & \frac{\hat{Y}_1(s)}{\hat{U}_2(s)} \\ \frac{\hat{Y}_2(s)}{\hat{U}_1(s)} & \frac{\hat{Y}_2(s)}{\hat{U}_2(s)} \end{bmatrix} \tag{7}$$

where ^ denotes estimation, Y_x and U_x are the Laplace transforms of the output and input signals, respectively. Suffixes 1 and 2 stand for aft and fore bodies, respectively.

The optimal transfer function order was achieved by using the *parsimony principle* which states that "the model should contain the smallest number of free parameters required to represent the true system adequately" (Soderstrom and Stoica 1989). The best results were obtained using four poles and three zeros for each transfer function in (7).

The fit criterion is calculated using the NRMSE metric:

$$Fit = 100(1 - NRMSE) \tag{8}$$

Fit is a percent value and varies between $-\infty$ (poor fit) to 100 (perfect fit) (Ljung 2019).

The fit criterion (8) is used to compare the accuracy of each identification strategy. It is given as a 2x2 matrix where each percent value corresponds to the fit metric for each transfer function element in (7).

Table 1 shows the fitting percent for each strategy. As can be noted, the third one clearly gives more accurate results than the other strategies.

4.3 *Model validation*

The model obtained with the third strategy was validated against a chirp signal with the same frequency

Table 1. *Fit* value for each element of the TFM in (7) for each identification strategy.

Strategy 1	Strategy 2	Strategy 3
$\begin{bmatrix} 4.38 & 22.04 \\ 7.05 & 26.59 \end{bmatrix}$	$\begin{bmatrix} 28.23 & 77.66 \\ -72.70 & 73.13 \end{bmatrix}$	$\begin{bmatrix} 80.96 & 77.82 \\ 74.89 & 77.05 \end{bmatrix}$

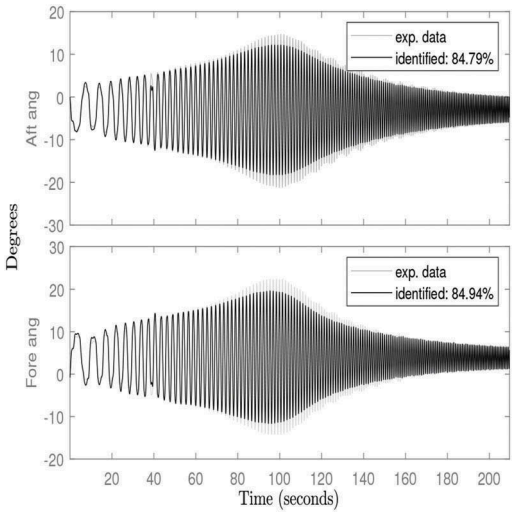

Figure 7. Comparison of modelled and experimental system.

sweep but with 69 N amplitude. Figure 7 shows the comparison between the experimental data output and the identified model output. It can be seen that the *Fit* value is above 84%.

5 CONCLUSIONS

A linear model was obtained using system identification techniques and experimental data. In order to do the identification, it was necessary to preprocess the data first. Several strategies were developed to get an accurate linear model. It was found that merging the data of all the recorded input and output signals and then estimating the transfer function with these data, gives the best results. The identified model was validated against a chirp signal with a different amplitude. The simulated response of the estimated linear model has a fidelity of 84% with this new signal.

ACKNOWLEDGEMENTS

This paper is based upon work supported by Science Foundation Ireland under Grant no. 13/IA/1886.

REFERENCES

Cummins, W. (1962). The impulse response function and ship motions. *Schiffstechnik 47*, 101–109.

Davidson, J., S. Giorgi, & J. V. Ringwood (2015). Linear parametric hydrodynamic models for ocean wave energy converters identified from numerical wave tank experiments. *Ocean Engineering 103*, 31–39.

Davidson, J., S. Giorgi, & J. V. Ringwood (2016). Identification of wave energy device models from numerical wave tank data-part 1: Numerical wave tank identification tests. *IEEE Trans. Sust. Energy 7*(3), 1012–1019.

de Almeida, A. & P. Moura (2007). Desalination with wind and wave power. In *NATO Sec. Sc. C. Env. Sec*., pp. 305–325.

Garcia-Violini, D., Y. Pena-Sanchez, N. Faedo, C. Windt, & J. Ringwood (2020, July). LTI energy-maximising control for the wave star wave energy converter: identification, design, and implementation. In *Proc. World Congress, IFAC*, Berlin, Germany, pp. to appear.

Giorgi, S., J. Davidson, M. Jakobsen, M. Kramer, & J. V. Ringwood (2019). Identification of dynamic models for a wave energy converter from experimental data. *Ocean Engineering 183*, 426–436.

Giorgi, S., J. Davidson, & J. V. Ringwood (2016). Identification of wave energy device models from numerical wave tank dataâ€"part 2: Data-based model determination. *IEEE Trans. Sust. Energy 7*(3), 1020–1027.

Ljung, L. (1999). *System Identification: Theory for the User* (Second ed.). Prentice-Hall.

Ljung, L. (2002, December). Identification for control: simple process models. In *Proc. of the 41st IEEE Conf. on Decision and Control*, pp. 4652–4657.

Ljung, L. (2009, July). Experiments with identification of continuous time models. In *Proc. of the 15th IFAC Symposium on System Identification*, Saint-Malo, France, pp. 1175–1180.

Ljung, L. (2010). Perspectives on system identification. *Annual Rev. in Control 34*(1), 1–12.

Ljung, L. (2019). *System Identification Toolbox for use with MATLAB: Reference (R2019b)*. Massachusetts, USA: The MathWorks, Inc.

Mocean Energy (2020). Mocean energy news. https://www.mocean.energy/wave-energy-news/. Accessed April 10, 2020.

O'Cathain, M., B. J. Leira, & J. Ringwood (2007). Modelling of multibody marine systems with application to wave-energy devices. In *Proc. of the 7th European Wave and Tidal Energy Conference*, Porto, Portugal.

Offshore Energy (2016). WECCA completes scaled wave energy device. https://www.offshore-energy.biz/wecca-completes-scaled-wave-energy-device-prize/. Accessed April 10, 2020.

Ozdemir, A. A. & S. Gumussoy (2017). Transfer function estimation in system identification toolbox via vector fitting. *IFAC-PapersOnLine 50(*1), 6232–6237.

Paparella, F., G. Bacelli, A. Paulmeno, S. E. Mouring, & J. V. Ringwood (2016). Multibody modelling of wave energy converters using pseudo-spectral methods with application to a three-body hinge-barge device. *IEEE Trans. Sust. Energy 7(*3), 966–974.

Paparella, F. & J. V. Ringwood (2017). Optimal control of a three-body hinge-barge wave energy device using pseudospectral methods. *IEEE Trans. Sust. Energy 8(*1), 200–207.

Ringwood, J. (2020, July). Wave energy control: status and perspectives 2020. In *Proc. World Congress, IFAC*, Berlin, Germany, pp. to appear.

Ringwood, J., G. Bacelli, & F. Fusco (2014, October). Energy-maximizing control of wave-energy converters: The development of control system technology to optimize their operation. *IEEE Control Syst. Mag. 34*(5), 30–55.

Seapower (2020). Seapower. http://www.seapower.ie/. Accessed April 10, 2020.

Soderstrom, T. & P. Stoica (1989). *System Identification*. Prentice-Hall.

Stansby, P., E. Carpintero Moreno, T. Stallard, & A. Maggi (2015). Three-float broad-band resonant line absorber with surge for wave energy conversion. *Renewable Energy 78*, 132–140.

Yemm, R., D. Pizer, C. Retzler, & R. Henderson (2012). Pelamis: Experience from concept to connection. *Phil. Trans. R. Soc. A. 370*, 365–380.